Electronic Supplementary Material (ESI) for Physical Chemistry Chemical Physics.

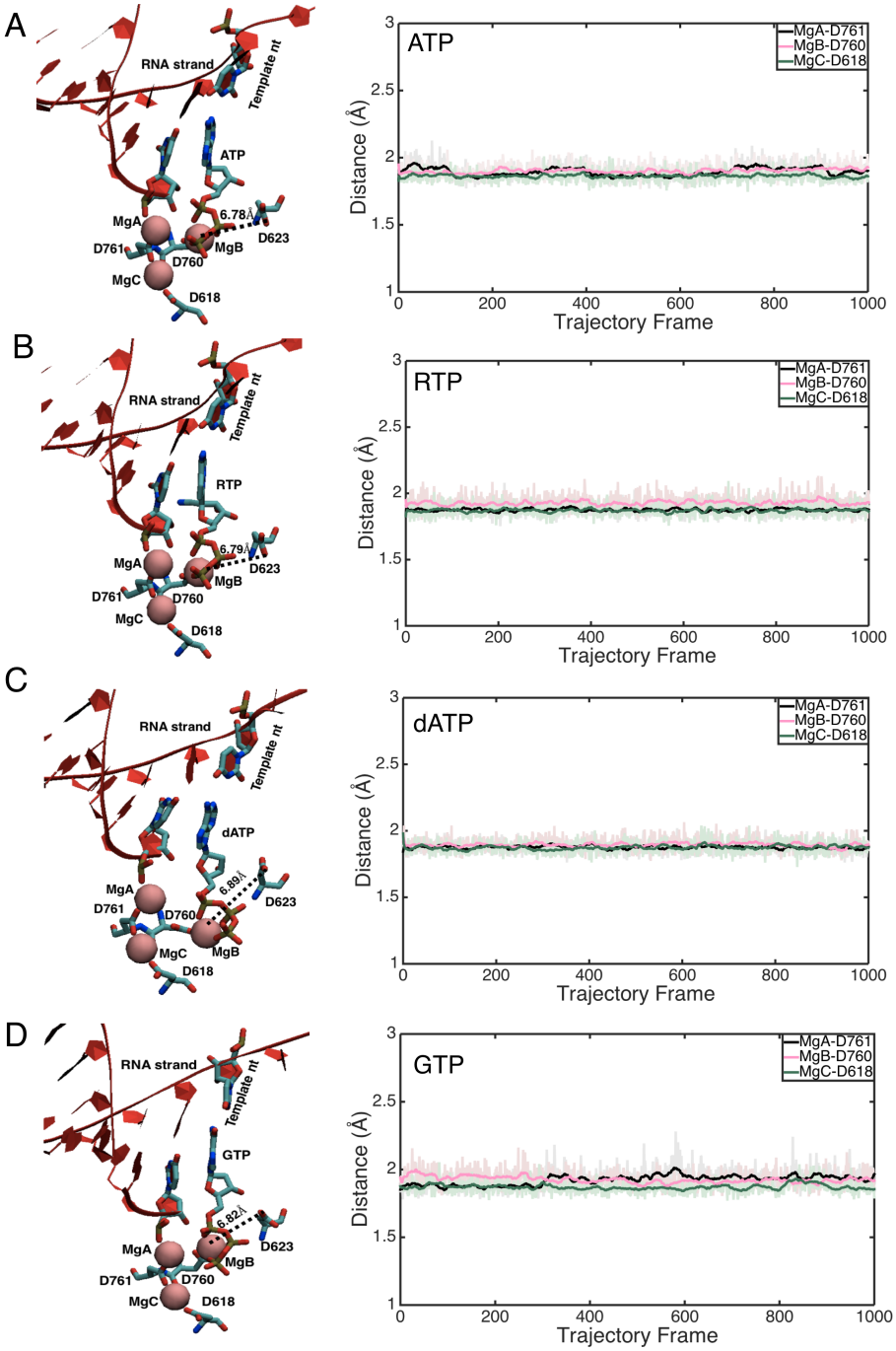

Figure S1. The distances measured between MgA, MgB, MgC and D761, D760, D618 from ensemble equilibrium simulations. The three magnesium ions were modeled according to version 1 of the PDB (7BV2) structure. The distances were measured between the magnesium ion (in pink spheres) and the atom OD1 of the aspartic acid residue, for the insertion state of the RdRp complex, bound with ATP (A), RTP (B), dATP (C), and GTP (D). In comparison, the distances between MgB and D623 are large, about 6.8-6.9 Å as labeled in all the above systems.

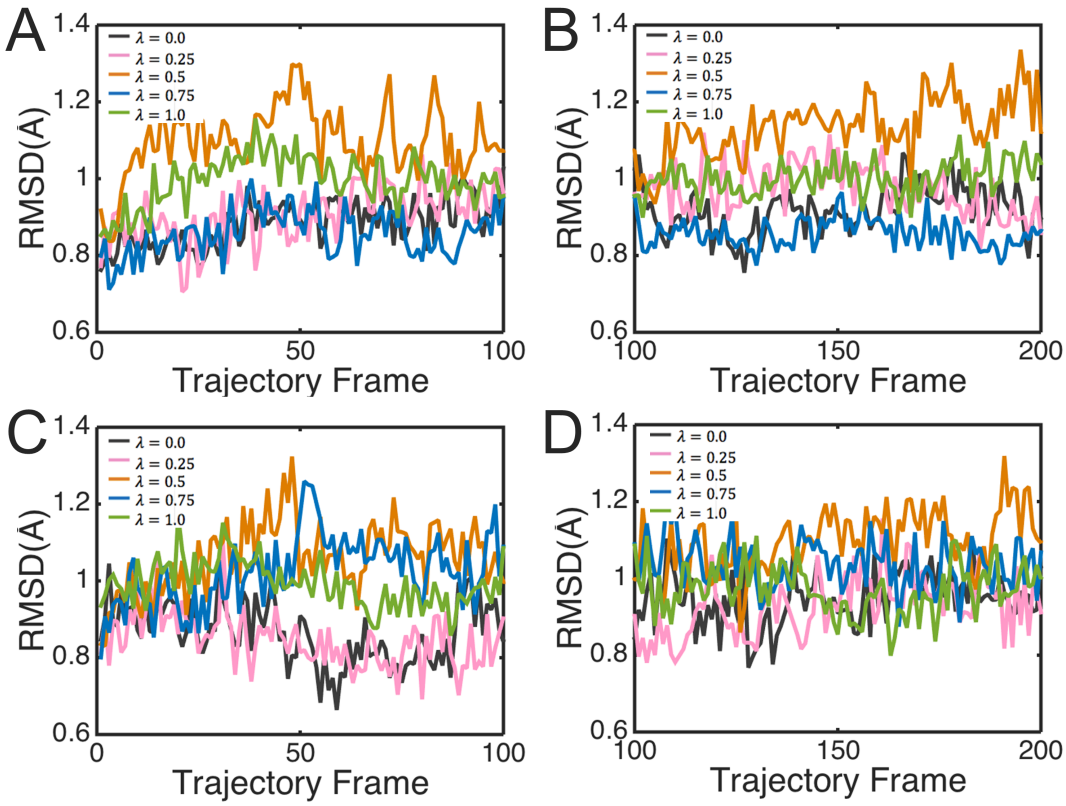

Figure S2. The RMSDs during 0-5 ns and 5-10 ns MD in five alchemical MD simulations with $\lambda = 0.0, 0.25, 0.50, 0.75, 1.0$, shown with 100 trajectory frames for each in the alchemical binding free energy calculation for the ATP insertion state. (A & B) The RMSD values of the fingers subdomain in SARS-CoV-2 RdRp during 0-5 ns (A) and during 5-10 ns MD simulations (B). (C & D) The RMSD values of the palm subdomain in SARS-CoV-2 RdRp during 0-5 ns (C) and during 5-10 ns MD simulations (D).

Closed state	ΔG_3(kJ/mol)	ΔG_1(kJ/mol)	ΔG_b(kcal/mol)
ATP	-75.83	-28.07	-11.42
RTP	-66.76	-28.89	-9.06
dATP	-67.83	-25.79	-10.06
GTP	-66.47	-31.08	-8.47

Table S1. The free energetics obtained from alchemical simulations for binding free energy calculations in SARS-CoV-2 RdRp with an NTP (ATP/RTP/dATP/GTP) bound in the closed or insertion state. The corresponding thermodynamic cycles [1, 2] for the calculations are presented in main Figure 2: ΔG_1 is the free energy converting dummy to NTP calculated in the free solution, and ΔG_3 is the free energy converting dummy to NTP conducted inside the protein complex. For each species, $\Delta G_b(NTP) = \Delta G_3 - \Delta G_1 + \Delta G_2$, with $\Delta G_2 = 0$ as the dummy is set to void in all cases.

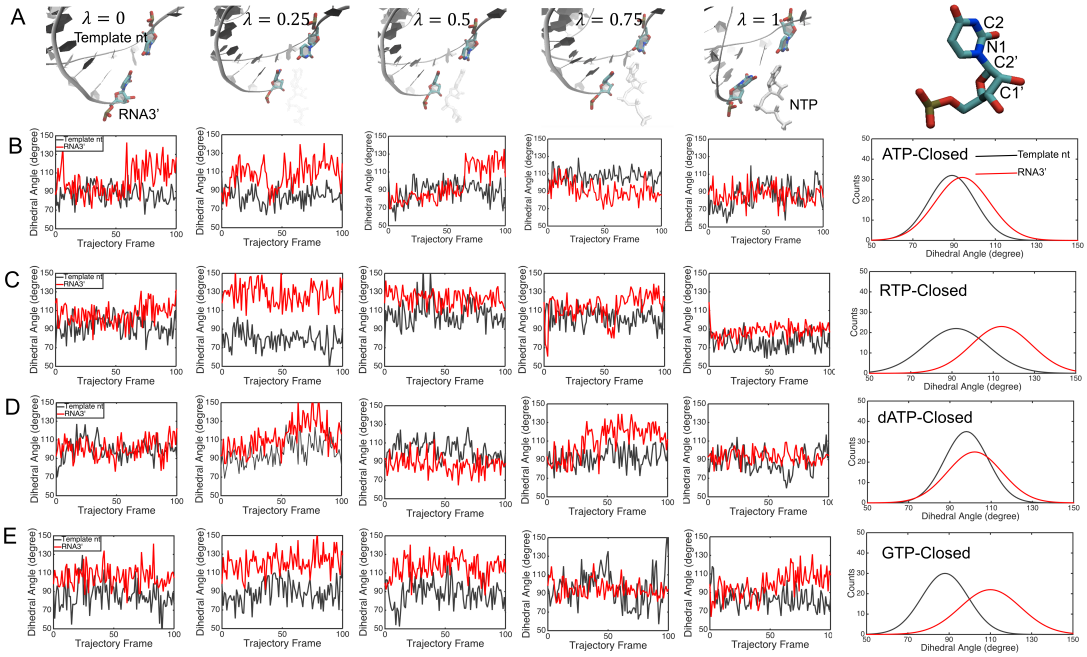

Figure S3. The dihedral angle distributions formed by four atoms of C1', C2', N1, C2 in template nt or RNA3' in $\lambda = 0,0.25,0.5,0.75,1$ of the alchemical simulation windows for SARS-CoV-2 RdRp with ATP, RTP, dATP, GTP bound in the closed active site (B/C/D/E) (*left*), respectively, histograms are shown on the right. The structures are shown in (A).

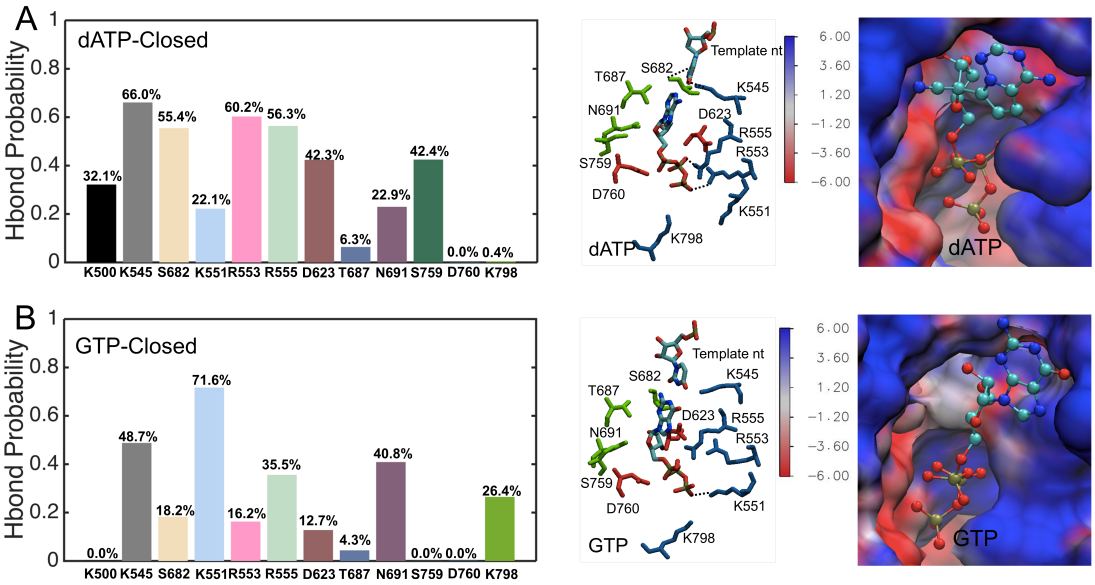

Figure S4. The hydrogen bonding association patterns between the active site amino acids and the non-cognate nucleotides modeled in closed state of SARS-CoV-2 RdRp, (A) for dATP and (B) for GTP, with the hydrogen bonding occupancies calculated from the ensemble equilibrium simulations (*left*) and the molecular views (*middle*), the electrostatic potential generated by solving the Poisson-Boltzmann equation using the APBS [3] in VMD [4] (*right*). The protein is colored based on the electrostatic potential from dark red (most negative) to dark blue (most positive), the values in the color bar are in units of $k_BT/|e|$.

.

	Vdw Energy (kJ/mol)	Ele energy (kJ/mol)	Polar solvation energy (kJ/mol)	Sasa energy (kJ/mol)	Binding energy (kcal/mol)
ATP	-75.7219	-851.1100	627.7952	-9.5211	-73.817
RTP	-79.4468	-885.6985	632.3792	-9.7640	-81.945
dATP	-77.7801	-833.4727	643.3111	-9.6039	-66.398
GTP	-78.3432	-796.1425	628.9265	-9.7646	-61.082

Table S2. The binding energetics calculated between insertion nucleotides ATP/dATP/GTP as well as nucleotide analogue RTP and SARS-CoV-2 complex by using gromacs g-mmpbsa with g-mmpbsa command default [5, 6].

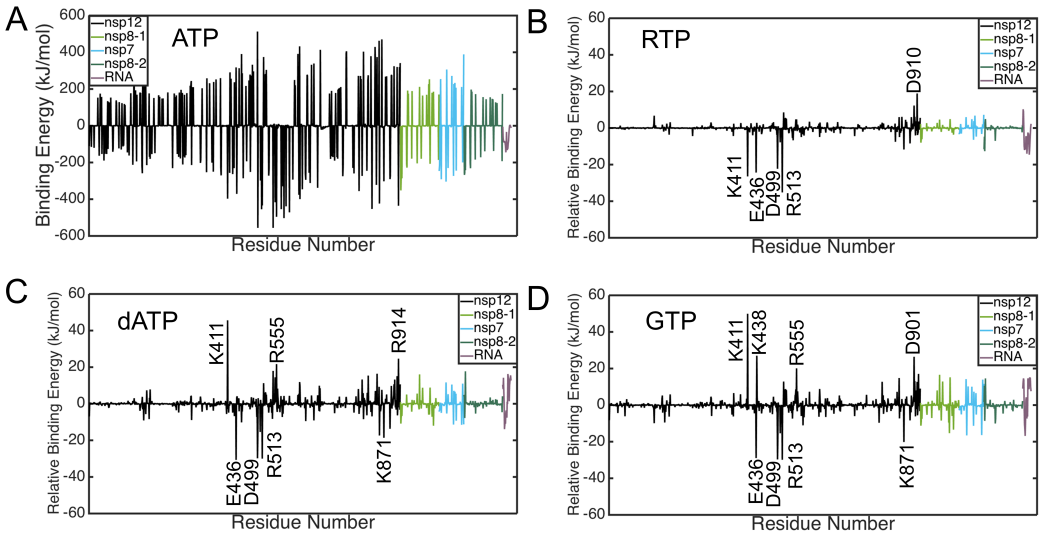

Figure S5. The total insertion nucleotide binding energetics (from MM/PBSA calculations) contributed by each amino acid and nucleotide in SARS-CoV-2 RdRp with (A) for ATP, (B) the relative binding energy for RTP according to ATP, (C) the relative binding energy for dATP, (D) the relative binding energy for GTP. The key residues contribute most to stabilization/destabilization are labeled.

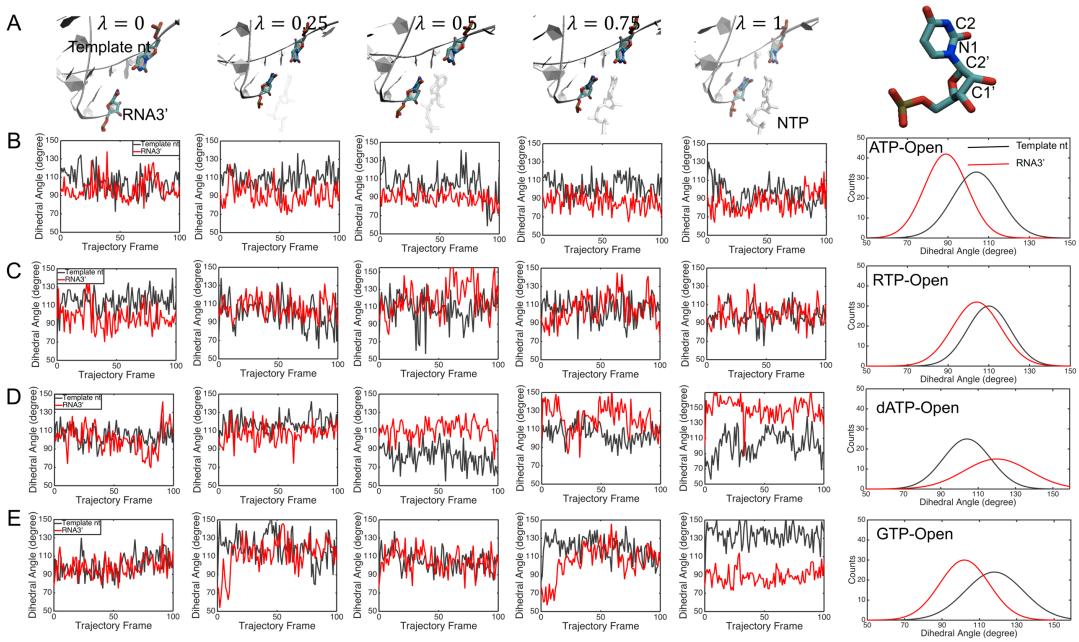

Figure S6. The dihedral angle distributions formed by four atoms of C1', C2', N1, C2 in template nt or RNA3' in the alchemical simulation windows $\lambda = 0,0.25,0.5,0.75,1$for SARS-CoV-2 RdRp with ATP, RTP, dATP, GTP initially bound in the open active site (B/C/D/E) (*left*), respectively, histograms are shown on the right. The structures are shown in (A).

Open state	ΔG_3(kJ/mol)	ΔG_1(kJ/mol)	ΔG_b(kcal/mol)
ATP	-64.95	-29.46	-8.49
RTP	-65.41	-28.78	-8.72
dATP	-55.12	-26.33	-6.98
GTP	-57.04	-28.52	-6.79

Table S3. The free energetics obtained from alchemical simulations for binding free energy calculations in SARS-CoV-2 RdRp with an NTP (ATP/RTP/dATP/GTP) bound in the open state. The corresponding thermodynamic cycles [1, 2] for the calculations are presented in main Figure 2: ΔG_1 is the free energy converting dummy to NTP calculated in the free solution, and ΔG_3 is the free energy converting dummy to NTP conducted inside the protein complex. Hence, $\Delta G_b(RTP) = \Delta G_3 - \Delta G_1 + \Delta G_2$, with $\Delta G_2 = 0$ due to the dummy is set as void in all these cases.

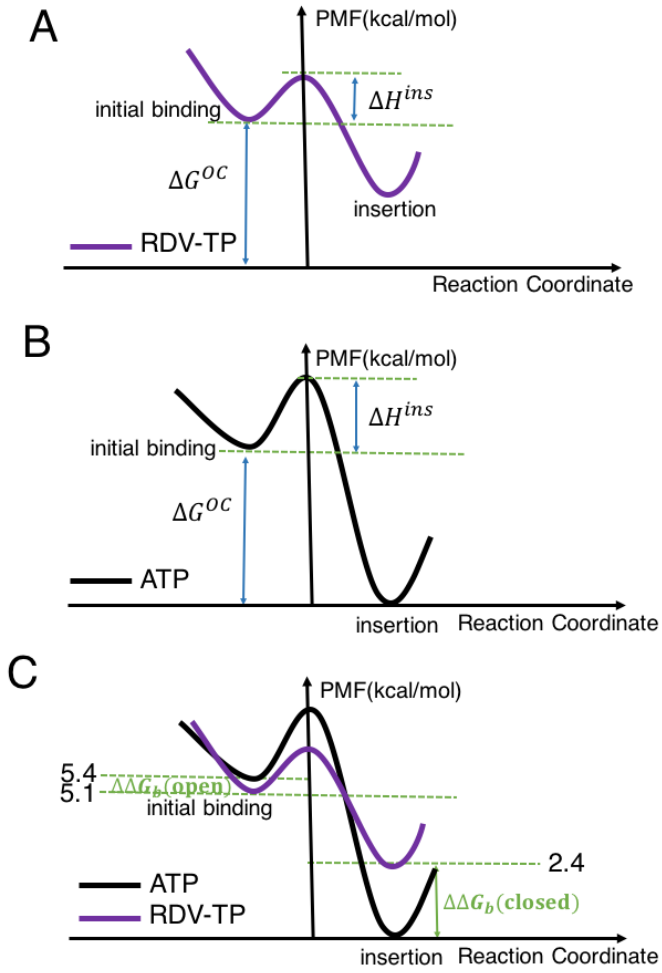

Figure S7. The schematic free energy profiles or potentials of mean force (PMFs) from the nucleotide initial binding to insertion of the cognate ATP and nucleotide analogue RDV-TP (or RTP). The PMFs of ATP and RTP are shown in black and purple curves, respectively. The two PMFs were calculated from the umbrella sampling simulation studies [7], as shown in (A and B), with ΔG^{oc} ~ 2.7 kcal/mol for RTP and ΔG^{oc} ~ 5.1 kcal/mol for ATP, and the insertion barrier ΔH^{ins} ~ 1.5 kcal/mol for RTP and ΔH^{ins} ~ 2.6 kcal/mol for ATP; without knowing the relative placement between the two PMFs yet. With current alchemical calculations, the two PMFs are able to be placed together as shown in (C). The relative binding free energies between RTP and ATP are calculated here as $\Delta\Delta G\_(open)$ (~ -0.2 kcal/mol) and $\Delta\Delta G\_(closed)$ (~2.4 kcal/mol), respectively, for the initial binding (open) and insertion states (closed).

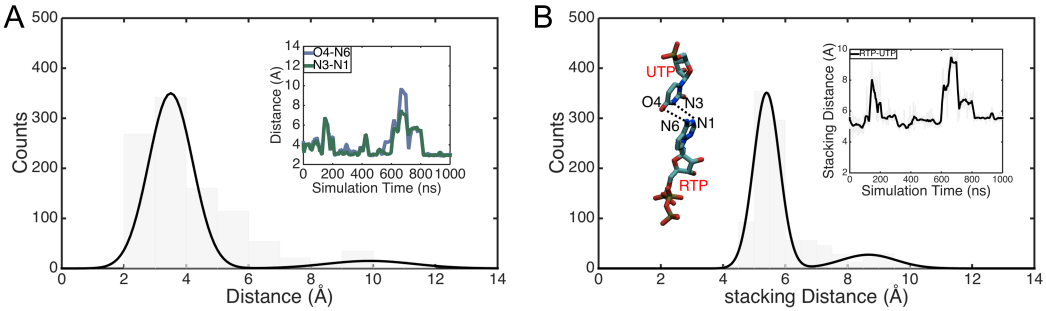

Figure S8. The histograms on measured distances between nucleotide RTP base and template nt (rUTP) base on atoms involved for base pairing (A) and base stacking (B). (A) is taken from main Fig 6B for comparison, while for (B) In the inset *right*, the stacking distances between rUTP base and template nt base. are shown over the simulation time. In the inset *left*, the structures of nucleotide RTP and the associating template rUTP are shown.

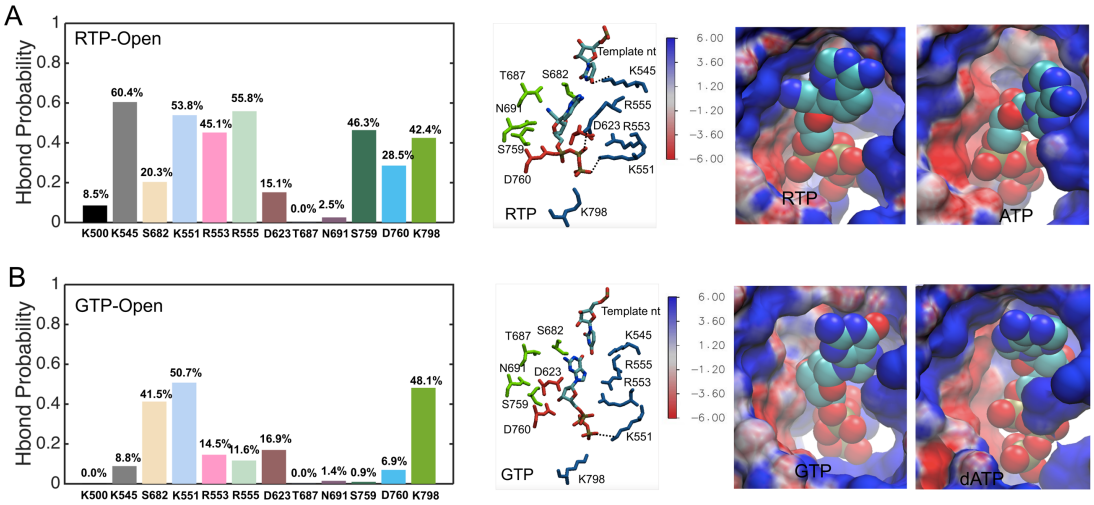

Figure S9. The hydrogen bonding association patterns between the active site amino acids and the nucleotide binding initially in open state of SARS-CoV-2 RdRp, (A) for RTP and (B) for GTP with the hydrogen bonding occupancies calculated from the ensemble equilibrium simulations (*left*) and the molecular views around the active site (*middle*), the electrostatic potential generated by solving the Poisson-Boltzmann equation using the APBS [3] in VMD along with RTP/ATP/GTP/dATP shown in vdW sphere (*right*). The protein is colored based on the electrostatic potential from low (negative) by red to high (positive) by blue, the values in the color bar are in units of $k_BT/|e|$.

	Vdw Energy (kJ/mol)	Ele energy (kJ/mol)	Polar solvation energy (kJ/mol)	Sasa energy (kJ/mol)	Binding energy (kcal/mol)
ATP	-68.9669	-906.1565	734.3293	-10.1123	-60.025
RTP	-83.0573	-853.1327	685.8072	-10.4425	-62.398
dATP	-67.9788	-948.9541	772.4889	-10.0580	-60.886
GTP	-69.6758	-832.1274	676.9507	-9.0651	-55.961

Table S4. The binding energetics calculated between initial binding nucleotides ATP/RTP/dATP/GTP and SARS-CoV-2 complex by using gromacs g-mmpbsa with g-mmpbsa command default [5, 6].

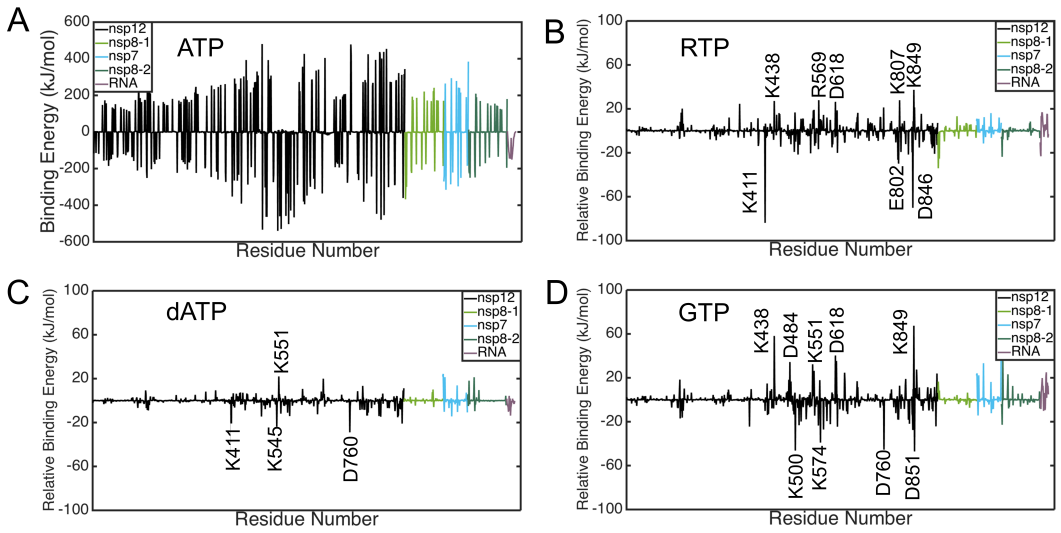

Figure S10. The total initial nucleotide binding energetics contributed by each amino acid and nucleotide in SARS-CoV-2 RdRp with (A) for ATP, (B) the relative binding energy for RTP according to ATP, (C) the relative binding energy for dATP, (D) the relative binding energy for GTP. The key residues contribute most to stabilization/destabilization are labeled.

Reference

1. Shirts MR, Pitera JW, Swope WC, Pande VS. Extremely precise free energy calculations of amino acid side chain analogs: Comparison of common molecular mechanics force fields for proteins. The Journal of chemical physics. 2003;119(11):5740-61.
2. Mobley DL, Chodera JD, Dill KA. On the use of orientational restraints and symmetry corrections in alchemical free energy calculations. The Journal of chemical physics. 2006;125(8):084902.
3. Jurrus E, Engel D, Star K, Monson K, Brandi J, Felberg LE, et al. Improvements to the APBS biomolecular solvation software suite. Protein Science. 2018;27(1):112-28.
4. Humphrey W, Dalke A, Schulten K. VMD: visual molecular dynamics. Journal of molecular graphics. 1996;14(1):33-8.
5. Baker NA, Sept D, Joseph S, Holst MJ, McCammon JA. Electrostatics of nanosystems: application to microtubules and the ribosome. Proceedings of the National Academy of Sciences. 2001;98(18):10037-41.
6. Kumari R, Kumar R, Consortium OSDD, Lynn A. g_mmpbsa A GROMACS tool for high-throughput MM-PBSA calculations. Journal of chemical information and modeling. 2014;54(7):1951-62.
7. Romero ME, Long C, La Rocco D, Keerthi AM, Xu D, Yu J. Probing remdesivir nucleotide analogue insertion to SARS-CoV-2 RNA dependent RNA polymerase in viral replication. Molecular Systems Design & Engineering. 2021;6(11):888-902.